

## Experimental and modeling studies of paper based methanol fuel cell

S. Lal<sup>a</sup>, V.M. Janardhanan<sup>a</sup>, M.Deepa<sup>b</sup>, K.C. Sahu<sup>a</sup>

<sup>a</sup>Department of Chemical Engineering, Indian Institute of Technology Hyderabad, Kandi, Sangareddy, 502 285, India

<sup>b</sup>Department of Chemistry, Indian Institute of Technology Hyderabad, Kandi, Sangareddy, 502 285, India

### Abstract

We develop a T-shaped paper based methanol (CH<sub>3</sub>OH) fuel cell consisting of two L-shaped paper strips, separated by a polyacryl amide (PAM) gel. With 0.25 ml of anolyte and catholyte, the cell delivers the maximum power density of 0.9 mW/cm<sup>2</sup> at 4M CH<sub>3</sub>OH. Hydrothermally synthesized N-rGO, NiCo<sub>2</sub>O<sub>4</sub> (NCO) and NCO@N-rGO are implemented as catalysts. Further, with 6 wt% N-rGO in NCO@N-rGO composite catalyst deposited at both electrodes, the cell delivers peak power density of 4.67 mW/cm<sup>2</sup> and maximum current density of 15.6 mA/cm<sup>2</sup>. This result shows an increase of 418% in the peak power density as compared to a cell without any catalyst. A mathematical model based on Butler-Volmer equation is formulated to predict the cell voltages at different experimental conditions. The numerically obtained dc-polarization curves agree well with the experimental measurements.

### Introduction

The market for portable electronics, such as laptops, mobile phones, digital watches, notebooks and point-of-care (POC) diagnostic devices for healthcare applications, has proliferated rapidly in the recent years, and has seen a remarkable growth in the last decade. With this, there has also been a manifold increase in the energy requirement, and thus the demand for power sources for these devices has been accelerating at the same rate. POC diagnostic devices such as glucometers, dengue detection kits, pregnancy detection kits are being commonly used for rapid diagnosis and analysis for medical applications (1,2,3). The operation of these devices requires low power (micro-nano watt), for a short duration and, usually Li-ion batteries are used. Thus, there is a need to develop mechanisms suitable for such applications. As an alternative to batteries, paper based devices, such as paper based fuel cells have attracted substantial attention in recent times, because of their low cost and ability to generate reasonable power suitable for micro-nano systems (MNS) and microelectromechanical systems (MEMS). The reason for choosing paper as the core substrate, can be attributed to the excellent properties of paper, e.g., porosity, capillarity and biodegradability. So far, several paper-based fuel cells have been reported and the highest power density attained till now is 103 mW/cm<sup>2</sup> (4). Different types of fuels such as formic acid, hydrazine hydrate, methanol, hydrogen peroxide, sodium percarbonate, hydrogen etc. have been employed, and elaborately characterized, but only a few reports have demonstrated its application. For example, Fraiwan and co-workers stacked four bacteria powered paper based batteries in series to illuminate an LED (5). However, the power density delivered by the microbial fuel cells is in  $\mu$ W/cm<sup>2</sup> with low open circuit voltage, OCV (< 1V). Therefore, in order to obtain high power densities, researchers have explored different paper based fuel cell

architectures and (above mentioned) fuels, and have come up with noteworthy and stable cell performances (6,7). A membraneless paper based fuel cell comprising of methanol-air fuel-oxidant system, with remarkable cell performance has been reported earlier, but the use Pt, Ru and Au (8), as catalysts, narrows down its ability to be placed as a cost-effective on-board energy source for MNS. Therefore, employing non-noble metals as catalysts such as Ni, Co, C, Cu, etc. could be an effective alternative. Recent reports on high catalytic activity of bimetallic oxides such as, nickel cobaltite ( $\text{NiCo}_2\text{O}_4$ ), in different morphologies, towards methanol, stimulates its implementation as a catalyst in our paper based fuel cell. Methanol has reportedly high cross-over and slow electro-oxidation rates (9). To cope with these limiting factors, a cell architecture with proton conducting gel/membrane separating the electrodes has been developed,  $\text{NiCo}_2\text{O}_4$  and  $\text{NiCo}_2\text{O}_4$ @N-rGO (nitrogen doped reduced graphene oxide) composite catalysts with high catalytic activity towards methanol, have been employed in the present work. Moreover, methanol has a high-energy density, it is cheap, easy to handle, store and easily available.

In the present work, we report the characterization of paper based methanol fuel cell. Whatman filter is the support/substrate for the cell;  $\text{KMnO}_4$  is used as the oxidant, because of its strong oxidation properties and high reduction potential (1.51 V). Polyacryl amide (PAM) gel impregnated with  $\text{H}_2\text{SO}_4$  is used as the gel/membrane, and  $\text{H}_2\text{SO}_4$  and  $\text{NaOH}$  are used as the electrolytes in the anolyte and catholyte. The cell performance is optimized with 2M, 4M and 6M  $\text{CH}_3\text{OH}$ .  $\text{NiCo}_2\text{O}_4$  and  $\text{NiCo}_2\text{O}_4$ @N-rGO are used as catalysts. A mathematical model based on the Butler-volmer equation is developed to predict the current densities of the paper based cell, for the first time, and the results are compared with the experimental results. In order to demonstrate the application of our paper cell, a series of two paper cells have been connected to illuminate an LED which continued to glow for more than 30 minutes. The cell has a fairly high regenerative ability for its current density when replenished with fresh reagents.

## Experimental

### Cell assembly:

The cell was assembled by placing two L-shaped paper strips at a distance of 0.2 cm and PAM gel was placed in between the strips as shown in Fig.1. The gel acts as a proton exchange membrane for transport of ions. The anolyte and catholyte were discharged on the short arm, each measuring 0.5 cm X 2.5 cm, as indicated in Fig 1.

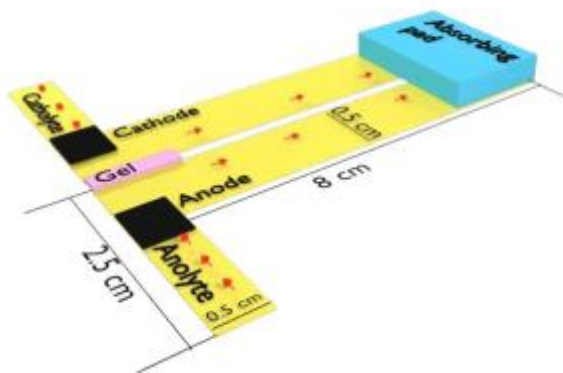


Figure 1: Schematic of paper based methanol fuel cell.

The short arm serves as the inlet, while long arm measuring, 8 cm X 0.5 cm, serves as the outlet for the products and excess and leftover reactants. The concentration of CH<sub>3</sub>OH was varied from 2M to 4M to 6M, in the anolyte containing 4M NaOH (electrolyte). The concentration of the catholyte was kept constant at 1M KMnO<sub>4</sub> and 4M H<sub>2</sub>SO<sub>4</sub>. Carbon cloth was cut into 0.5 cm X 0.5 cm and served as the electrodes, and steel plates were used as the current collectors. The PAM gel was placed between the electrodes, such that it is in contact with both anode and cathode. An absorbent pad was placed at the end of the long strip to absorb the downstream flow. The whole cell assembly was placed on a glass slide.

Preparation of PAM gel/membrane, NiCo<sub>2</sub>O<sub>4</sub> (NCO) hollow microspheres and NCO@N-rGO~composite:

Two grams of acrylamide were dissolved in 10 ml of DI water and the resulting solution was stirred at 500 rpm and heated at a temperature of 90 °C for 10 minutes, until the solution was completely homogeneous. Post this, 6 mg of ammonium persulphate was added to the above solution and was heated at this temperature with continuous stirring for 30 minutes. Ammonium persulphate provides the free radicals for the preparation of the polyelectrolyte and initiates the polymerization reaction. Once the solution was sufficiently viscous, the stirring was stopped and it was left to cool down at room temperature. After this, a solution of 2M H<sub>2</sub>SO<sub>4</sub> was added to the resultant gel, and this was left at room temperature for 4-5 hours. The H<sub>2</sub>SO<sub>4</sub> gets attached to the polymer chain of acrylamide by hydrogen bonding and H<sup>+</sup> ion acts as the mobile ion within the polymeric network, giving rise to a combination of ions and polymer chain, known as polyelectrolyte membrane/gel. This final product was PAM gel and serves as the medium of transport for the ions between the electrodes. The hydrothermal synthesis of hollow micro-spheres of NiCo<sub>2</sub>O<sub>4</sub> was done according to the procedure described elsewhere (10). The preparations of nitrogen doped graphene oxide (N-GO) and N-rGO were done according to the procedure described elsewhere (11). For the synthesis of NCO@N-rGO composite, three different weights of N-GO, i.e., 75 mg, 100 mg and 125 mg, were taken, and added to the solutions of Ni(NO<sub>3</sub>)<sub>2</sub>.6H<sub>2</sub>O and Co(NO<sub>3</sub>)<sub>2</sub>.6H<sub>2</sub>O, prior to the hydrothermal synthesis, as reported above (10). Thus, three different composites with varying content of N-rGO were obtained and the final products had 6 wt%, 8 wt% and 10 wt%, N-rGO in the composite.

## Results and discussion

CH<sub>3</sub>OH- KMnO<sub>4</sub> fuel-oxidant pair provides a theoretical open circuit voltage (OCV) of 2.32 V. The best cell performance is achieved by optimizing the CH<sub>3</sub>OH concentration in the anolyte. The fuel concentration is varied as 2M, 4M and 6M with 4M NaOH, while the concentration of the catholyte was kept constant, i.e., 1M KMnO<sub>4</sub> and 4M H<sub>2</sub>SO<sub>4</sub>. Fig 2a depicts the dc-polarization curves obtained at different fuel concentrations and the best cell performance was obtained at 4M CH<sub>3</sub>OH, while at 2M and 6M CH<sub>3</sub>OH the cell performances were low. Fig 3a represents the current sustainability of a fresh cell with 4M CH<sub>3</sub>OH with respect to time, and it is inferred that the cell can sustain its current density up to 2.5 mA/cm<sup>2</sup>, for about 15 minutes. The initial monotonous decrease in the current density is expected because of the consumption of the reactants on the electrodes. Moreover, when the same paper cell was dried out completely, and reused by replenishing anolyte and catholyte, it could still deliver a steady current density of

1mA/cm<sup>2</sup>. Based on the above findings it can be inferred that paper has an excellent absorption property and can hold the reagents within it for an appreciable period of time. This also demonstrates the self-pumping and self- transportation of fluids within the paper. As a result of this study, the CH<sub>3</sub>OH concentration was fixed at 4M in rest of the experiments.

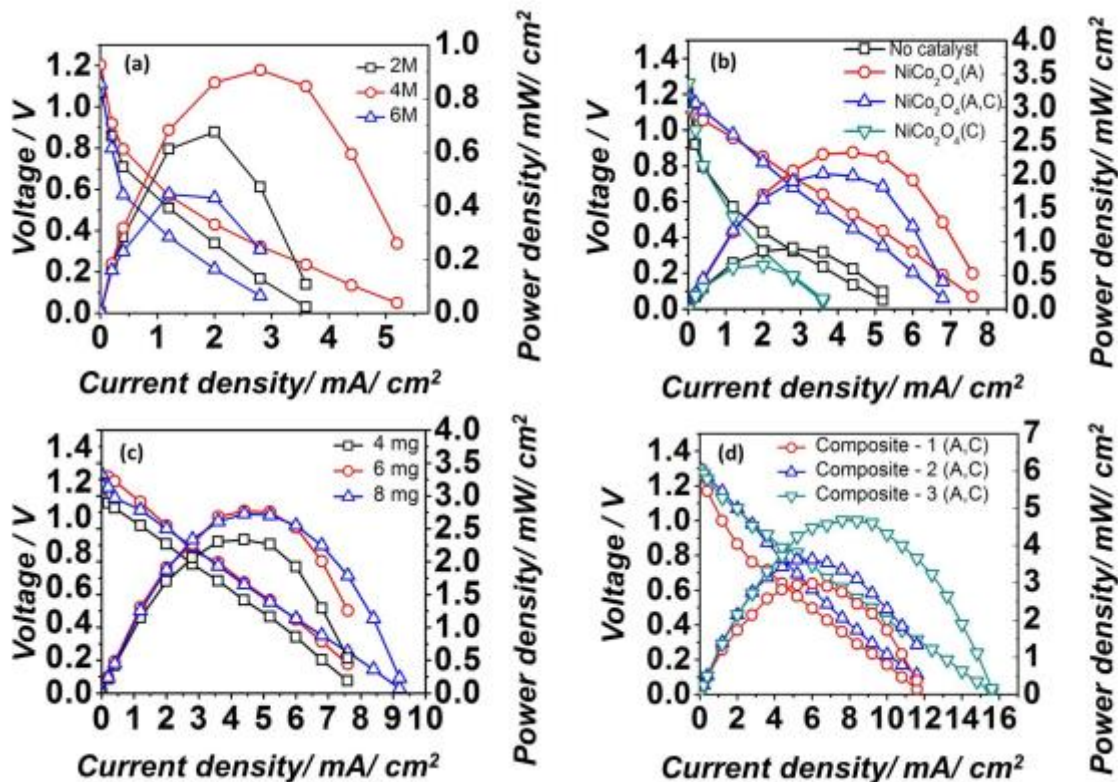


Figure 2: Cell performances with (a) different fuel concentrations in 4M NaOH (b) NiCo<sub>2</sub>O<sub>4</sub> as catalyst in various electrode combinations. (c) various NiCo<sub>2</sub>O<sub>4</sub> loadings, only at anode. (d) NCO@N-rGO with different wt% of N-rGO, composite 1- 6 wt%, composite 2- 8 wt%, composite 3- 10 wt% N-rGO, with 4M CH<sub>3</sub>OH + 4M NaOH as the anolyte and 1 M KMnO<sub>4</sub> + 4 M H<sub>2</sub>SO<sub>4</sub> as the catholyte.

Recently, nickel cobaltite, a binary metal oxide of Ni and Co, has been reported in different morphologies and its catalytic activity towards methanol oxidation has been studied elaborately. In our work, we have employed porous hollow microspheres of NiCo<sub>2</sub>O<sub>4</sub> and composites of NCO@N-rGO, and studied their effects on the cell performance, as shown in Fig 2(b)-(c). NCO was deposited on each of the electrodes (anode and cathode) separately, and then on both the electrodes. Fig 2(b) depicts the dc-polarization curves for different electrode combinations, and it is implicated that the maximum power density (MPD) of 2.3 mW/cm<sup>2</sup> was attained when NCO was present only at the anode. It is noteworthy that whenever, the catalyst was present at the anode, the activation losses (as seen in the dc-polarization curves), is less as compared to when the catalyst is absent at the anode. The cell performance was also studied at different NCO loadings, and the MPD of 2.77 mW/cm<sup>2</sup> was obtained at 6 mg of NCO, when present only at the anode, as shown in Fig 2(c). These findings lead us to the conclusion that NCO can effectively improve the methanol oxidation and thus enhance the cell

performance. To further improve the cell performance, composite catalyst NCO@N-rGO containing various wt% of N-rGO was deposited on both the electrodes, and the cell performances were studied. Composite 3, which has 10 wt% N-rGO in the composite delivers the MPD of 4.67 mW/cm<sup>2</sup>, as shown in Fig 2(d). This indicates that the combined effects of enhanced surface area, conductivity and more active sites present in N-rGO and the rich electroactive sites, porous surface of hollow microspheres of NiCo<sub>2</sub>O<sub>4</sub>, played a key role in accelerating the reaction kinetics at both anode and cathode.

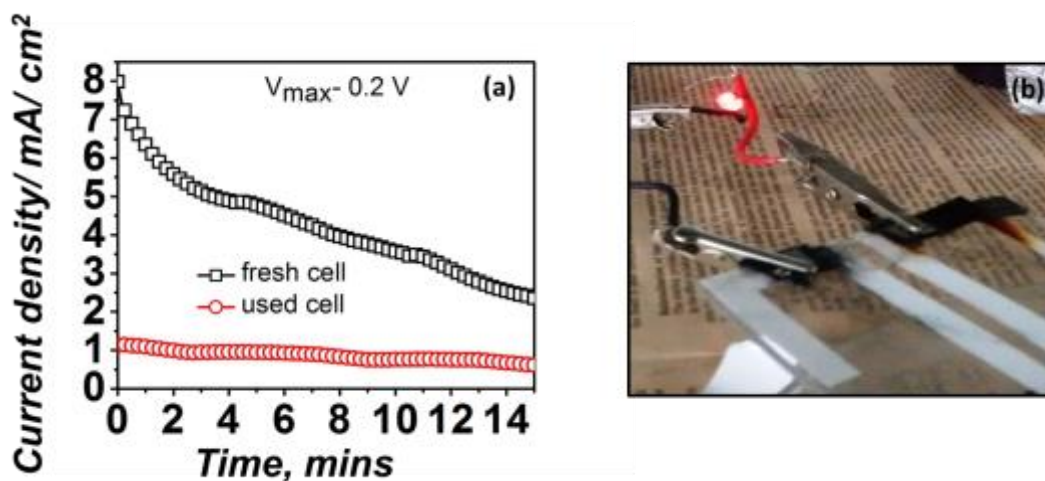


Figure 3. (a) Cell sustainability at 4M CH<sub>3</sub>OH and 1M KMnO<sub>4</sub> in 4M H<sub>2</sub>SO<sub>4</sub> with V<sub>max</sub>-0.2V. (b) Paper based methanol fuel cells illuminating an LED

A demonstration of the cell application is shown in Fig 3(b), where two paper cells were connected in series and a 3mm LED bulb served as the load. Once the anolyte and catholyte were discharged and reached the electrodes, the LED started glowing and continued to glow for nearly 30 minutes. This clearly proves that our paper cell can provide the sufficient power density for the required time, to power MNS, cost effectively.

A mathematical model using Butler-Volmer equation has been used to predict the cell voltages at experimental current densities, at different CH<sub>3</sub>OH concentrations in the anolyte and the catholyte concentration was kept constant. The exchange current densities at the anode and cathode vary as a function of fuel and oxidant concentration. The set of non-linear equations (eqn 1-3) was solved simultaneously in MATLAB using a non-linear function solver, *fsolve*. The numerically obtained dc polarization curves agree well with those obtained from the experimental measurements, as shown in Fig 4. The following equations have been used in the model.

$$E_{\text{cell}} = E_{\text{rev}} - (\eta_{\text{anode}} + \eta_{\text{cathode}} + \eta_{\text{ohm}} + \eta_{\text{leakage}}) \quad (1)$$

$$i = i_a \cdot \text{CH}_3\text{OH} \cdot \text{NaOH} \cdot \left\{ \exp \left[ \frac{\alpha F \eta_{\text{anode}}}{RT} \right] - \exp \left[ \frac{-\alpha F \eta_{\text{anode}}}{RT} \right] \right\} \quad (2)$$

$$i = i_c \cdot \frac{\text{KMnO}_4 \cdot \text{H}_2\text{SO}_4}{1 + \text{CH}_3\text{OH}^a \cdot \text{NaOH}^b} \cdot \left\{ \exp \left[ \frac{\alpha F \eta_{\text{cathode}}}{RT} \right] - \exp \left[ \frac{-\alpha F \eta_{\text{cathode}}}{RT} \right] \right\}, \quad (3)$$



$$\eta_{\text{leakage}} = \eta_{\text{leakage\_max}} (1 - i/i_{\text{max}}) \quad (4)$$

$$\eta_{\text{ohm}} = i.R_{\text{ohm}} \quad (5)$$

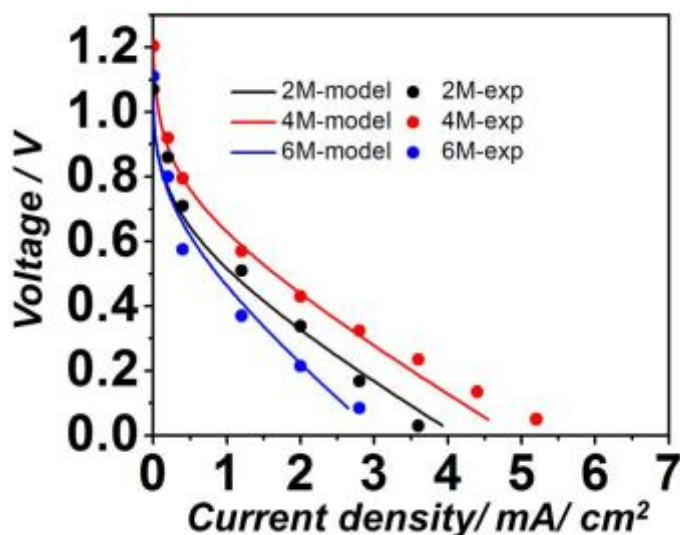


Figure 4. Dc-polarization curves at different CH<sub>3</sub>OH concentration predicted by the mathematical model.

### Concluding remarks

In this work, we have presented the development, working and characterizations of a paper based methanol fuel cell. The electrolyte is a mixture of varying concentrations of (2M, 4M and 6M) CH<sub>3</sub>OH and 4M NaOH. The catholyte is a mixture of 1M KMnO<sub>4</sub> and 4M H<sub>2</sub>SO<sub>4</sub>, and is kept constant through all the experiments. PAM gel serves as the medium of ion transportation between the electrodes and also prevents the cross-over of the fuel and oxidant. The cell delivers an MPD of 0.9 mW/cm<sup>2</sup> at 4M CH<sub>3</sub>OH and provides a current density of 2.5 mA/cm<sup>2</sup> even after 15 minutes of operation. This indicates the excellent absorption property paper, and its ability to hold the reagents within the system for a long time. In order to improve the cell performance and obtain a high-power density, hydrothermally synthesized hollow microspheres of NiCo<sub>2</sub>O<sub>4</sub> and composite of NiCo<sub>2</sub>O<sub>4</sub> and N-rGO, namely, NCO@N-rGO, have been employed as catalysts, in various loadings and electrode combinations. The best cell performance was assessed based on the MPD delivered by the cell. The MPD obtained with 6 mg NiCo<sub>2</sub>O<sub>4</sub> deposited at the anode, was 2.77 mW/cm<sup>2</sup>. The cell delivered MPD of 4.67 mW/cm<sup>2</sup> with 4 mg of NCO@N-rGO containing 10 wt% of N-rGO, deposited at both the electrodes, at 4M CH<sub>3</sub>OH. Two paper cells were stacked in series to illuminate a 3mm LED, which continued to light up for about 30 minutes. In addition to this, a kinetic model based on the Butler-Volmer equation was formulated to predict the current densities of the paper at different cell voltages and at different fuel concentrations. The cell performance as obtained from the model matched well with that obtained through the experimental characterizations of the cell. Thus, the present paper based methanol fuel cell can be used as an energy providing source for MNS and MEMS in a cost effective way. The miniaturized versions of these paper cells can be an onboard energy source for portable electronic devices.

## References

1. S. Lal, V. M. Janardhanan, M. Deepa, A. Sagar, and K. C. Sahu. *Journal of The Electrochemical Society*, **162**, F1402–F1407, (2015).
2. J. Esquivel, F. Del Campo, J. G. de la Fuente, S. Rojas, and N. Sabate.. *Energy & Environmental Science*, **7**, 1744–1749, (2014).
3. Z. L. Wang and W. Wu. *Angewandte Chemie International Edition*, **51**, 11,700–11,721, (2012).
4. J.P. Esquivel, J.R. Buser, C.W. Lim, C. Domínguez, S. Rojas, P. Yager, N. Sabaté, *J. Power Sources*, **342**, 442-451, (2017).
5. A. Fraiwan, S. Choi. *Phys. Chem. Chem. Phys.* **16** (47), 26288–26293, (2014).
6. S. S. Chen, C.-W. Hu, I.-F. Yu, Y.-C. Liao, J.-T. Yan. *Lab Chip*, **14** (12), 2124–2130, (2014).
7. S. M. Mousavi Ehteshami, M. Asadnia, S. N. Tan, S. H. Chan. *J. Power Sources*, **301**, 392–395, (2016).
8. J. Esquivel, F. Del Campo, J. De La Fuente, S. Rojas, N. Sabate. *17th International Conference on Miniaturized Systems for Chemistry and Life Sciences, MicroTAS*, 1251–1253, (2013).
9. H. Liu, C. Song, L. Zhang, J. Zhang, H. Wang, D.P. Wilkinson, *J. Power Sources*, **155**, 95-110, (2006).
10. G. Chen, Y. Gao, and H. Zhang, *RSC Advances*, **6**, 30488-30497, (2016).
11. M. Du, J. Sun, J. Chang, F. Yang, L. Shi, L. Gao, *RSC Advances*, 42412-42417, (2014).